processes

MDPI

Article

Influence of Compound Additives on Sulfur Fixing Performance of Sorbent Based on Steel Slag at High Temperatures

Jianbing Zhao [1,2,*], Qiaowen Yang [1], Xin Wen [1] and Meihui Li [1]

[1] School of Chemical and Environmental Engineering, China University of Mining and Technology-Beijing, Beijing 100083, China; abcyqw@sina.com (Q.Y.); sanbovision@163.com (X.W.); lmh17853989803@163.com (M.L.)
[2] Heilongjiang Forestry Vocation-Technical College, Mudanjiang 157011, China
* Correspondence: bqd1700303022@student.cumtb.edu.cn

Abstract: Steel slag is modified with additives to improve its high-temperature sulfur-fixing performance. The effects of sodium lignosulfonate, NaCl, KNO_3 and MnO_2 on the sulfur fixing performance of steel slag were explored after the ideal calcium–sulfur ratio of steel slag was established to be 2.5. An orthogonal experiment was used to explore the primary and secondary impacts of different additives on the sulfur fixing efficiency. The optimal factor level combination was identified to be 8% sodium lignosulfonate, 1% NaCl, 5% MnO_2, and 7% KNO_3, with a maximum sulfur fixing efficiency of 70.81%. According to XRF analysis, the sulfur-fixing effect of steel slag with additives was clearly superior to that of steel slag without additives. According to an XRD analysis, the diffraction peak of sulfur-fixing products of steel slag with additives was significantly improved, resulting in a high-temperature resistant phase that prevented sulfur-fixing products from degrading. According to SEM research, the steel slag with additives produced an interface that was conducive to gas–solid interaction in the sulfur fixation process, and sulfur fixed ash of modified steel slag exhibited the surface morphology of a high temperature resistant phase.

Keywords: steel slag; coal combustion; sulfur fixing agent; sulfur fixation efficiency; orthogonal experiments

Citation: Zhao, J.; Yang, Q.; Wen, X.; Li, M. Influence of Compound Additives on Sulfur Fixing Performance of Sorbent Based on Steel Slag at High Temperatures. *Processes* **2022**, *10*, 1272. https://doi.org/10.3390/pr10071272

Academic Editor: María Victoria López Ramón

Received: 9 May 2022
Accepted: 26 June 2022
Published: 28 June 2022

1. Introduction

Coal is used in large quantities, releasing nitrogen oxides and sulfur oxides in the power, building materials, iron and steel, and chemical industries. With the shift in economic development mode and the promotion of energy conservation and emission reduction, demand for coal has slowed, but pollution from coal-consuming companies remains severe [1]. The use of sulfur fixing agents [2] is a key coal combustion technique for controlling SO_2 emissions [3]. The development of low-cost and efficient sulfur-fixing agents for coal combustion is an important research area in clean coal technology.

Commonly used sulfur fixing agents [4,5] are $CaCO_3$ [6,7], $Ca(OH)_2$ and CaO [8], and non-calcium-based sulfur fixing agents have limited application in coal combustion sulfur fixing due to high prices. Calcium-containing solid waste, such as calcium carbide slag, red mud [9], white mud, fly ash, steel slag, etc. as sulfur fixing agents, is an effective way to utilize the resource of solid waste [10], and the development of alkali-based industrial solid waste [11] as a sulfur fixing agent can reduce the cost of sulfur fixing agent and reduce the land occupation of waste and environmental pollution [12]. Calcium-based sulfur fixing agents and solid waste used directly as a sulfur fixing agent, due to high temperature sintering and the decomposition of sulfur fixing products, lead to a low calcium utilization rate.

Auxiliary agents can increase the surface characteristics and pore structure of sulfur-fixing agents, as well as delay and limit the decomposition of sulfur-fixing products [13]. They can also catalyze sulfur-fixing reactions and combustion. Sulfur-fixing additives

such as NaCl and Na_2CO_3 are frequently used to modify sulfur-fixing agents [14], and sodium salts can form a low eutectic with calcium-based sulfur-fixing agents to promote ionic diffusion of reactants, which facilitates the formation of high surface area pores and improves sulfur-fixing agent reaction activity. Metal oxides, such as CeO_2, TiO_2, MnO_2, CuO and others [15], are used as additives in calcium-based sulfur-fixing agents in the coal combustion sulfur-fixing reaction process, not only to promote the sulfur-fixing reaction but also to improve fuel efficiency [16].

Steel slag is a type of industrial solid waste produced during the manufacturing of steel. Steel slag, as a solid waste, depletes land resources and pollutes the environment [17,18]. Steel slag is primarily used in road construction, building materials [19], cement production [20], and agriculture. Steel slag is used as an aggregate in asphalt mixtures for road construction, and steel slag powder is used as a hot melt in ceramic products and water treatment agents [21], and also as a soil conditioner [22,23]. Steel slag consumption has steadily shifted from crude to fine resource use in recent years, indicating a trend [24,25].

Steel slag is primarily composed of CaO, SiO_2, MgO, Al_2O_3, FeO, MnO, and other elements [26,27]. Steel slag is high in CaO and MgO, and finely ground steel slag powder slurry has a high alkalinity and is commonly used as a wet flue gas desulfurization absorber [28]. To increase the sulfur-fixing efficiency and reactivity, as well as to limit the sintering and decomposition of sulfur-fixing products in the high temperature sulfur-fixing process, the use of steel slag as a sulfur-fixing agent for coal combustion requires additive modification. In this paper, the use of additive-modified steel slag as a coal-fired sulfur-fixing agent to enhance the chemical activity of steel slag provides a new utilization value for steel slag, replacing traditional calcium-based sulfur-fixing agents such as limestone and thus saving mineral resources. This paper uses orthogonal experimental design to optimize the additive ratio and determine the maximum sulfur fixing efficiency and examines the high-temperature sulfur-fixing efficiency of steel slag and the sulfur-fixing mechanism of modified steel slag.

2. Materials and Methods

2.1. Sulfur Fixation Experiment

The experimental coal samples were chosen from Taiyuan coal, and the proximate analysis of coal samples is presented in Table 1. The coal samples were ground to less than 75 μm and left aside; the steel slag was ground to less than 75 μm and set aside (Table 2). As sulfur-fixing additives, KNO_3, NaCl, MnO_2, and sodium lignosulfonate were used. A certain amount of sulfur-fixing additives and steel slag was ground and mixed, and then according to a certain calcium–sulfur mole ratio, the Taiyuan coal was ground and mixed and put into a porcelain boat in a tube furnace and was rapidly heated to 1000 °C. The air compressor was started to pass a 2.5 $L \cdot min^{-1}$ flow of air, and was pushed into the combustion boat with the mixed coal samples, heated for 20 min, then taken out of the combustion boat for cooling. The sulfur fixation experiments were completed and the sulfur fixation ash was obtained. The sulfur fixation process is shown in Figure 1.

Table 1. Proximate and heating value analysis of samples.

Sample	Proximate Analysis w_{ad}/%				Sulfur Analysis w_{ad}/%	BCV/MJ·Kg^{-1}
	M	A	V	FC *	S_t	$Q_{b,ad}$
Taiyuan coal	1.38	36.42	25.99	36.26	2.50	20.188

Note: M—moisture; V—volatile; A—ash; FC—fixed carbon; BCV—bomb calorific value; ad—air dry basis; *—by difference.

Table 2. Chemical composition analysis of steel slag.

Composition	**CaO**	**Fe_2O_3**	**SiO_2**	**MgO**	**MnO**	**Al_2O_3**	**P_2O_5**	**TiO_2**
Content/%	42.83	25.34	16.79	3.52	3.44	3.15	1.87	1.40
Composition	**Cr_2O_3**	**Na_2O**	**BaO**	**K_2O**	**SrO**	**WO_3**	**Ag_2O**	**ZnO**
Content/%	0.486	0.199	0.119	0.0775	0.0473	0.0266	0.0237	0.0219

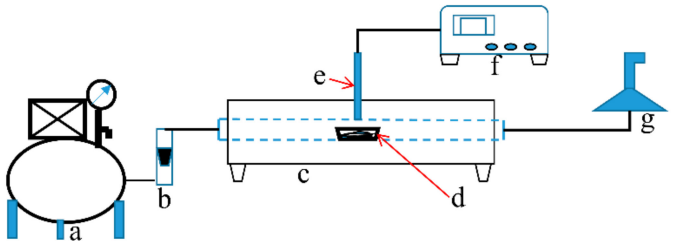

Figure 1. Schematic diagram of sulfur fixation equipment. a: Air compressor; b: Flow-meter; c: Tube furnace; d: Combustion boat; e: Thermocouple; f: Thermostat; g: Exhaust system.

2.2. Determination of Sulfur-Fixing Efficiency

The determination of sulfur in ash was performed using the GB/T215-2003 methodology to investigate sulfate sulfur concentration. The exact procedure for determining the mass of $BaSO_4$ was as follows: the ash was wetted and mixed with a certain concentration of concentrated hydrochloric acid and then boiled before being filtered to obtain the filtrate. The filtrate was transformed into barium sulfate precipitate, and was then filtered to obtain the filter paper with the precipitate. The filter paper was put in the muffle furnace to obtain the $BaSO_4$ precipitate; the mass of $BaSO_4$ was then weighed and calculated. The sulfur-fixing efficiency was calculated by dividing the mass of sulfur in the ash by the mass of sulfur in the matching coal sample, using the formula below:

$$\eta = \frac{m_1 \times w_1}{m_0 \times w_s} \times 100, \quad (1)$$

where, η is the sulfur fixation efficiency, %; m_1 is the mass of $BaSO_4$ precipitation measured, g; m_0 is the mass of raw coal, g; w_1 is the mass fraction of sulfur in $BaSO_4$, %; w_S is the sulfur content of raw coal, %.

2.3. Instruments for Experimentation and Analysis

A silent oil-free air compressor (TYW-1), a high temperature combustion tube furnace (SRJK-2-13), a muffle furnace (SX2), an electronic analytical balance (BSA124S), an industrial analyzer (MAC-400), and other items were made available.

X-ray fluorescence spectroscopy was used to determine the major elemental compositions of steel slag and tempered modified steel slag sulfur-fixing ash (XRF, PFX-235, Thermo, USA). X-ray diffraction (XRD, X'Pert Pro, PANalytical B.V., Holland) was used to study the primary crystalline phases found in steel slag and sulfur fixation ash. Scanning electron microscopy was used to examine the microscopic morphology of steel slag and sulfur-fixing ash (SEM, S-4800, Hitachi, Japan).

3. Results and Discussion

3.1. Determination of Calcium-Sulfur Mole Ratio

The impact of the calcium–sulfur mole ratio on the sulfur-fixing efficiency of steel slag is shown in Figure 2. Figure 2 shows that the sulfur fixation efficiency rises as the calcium–sulfur ratio grows, that the sulfur fixation efficiency of steel slag is the first to develop more quickly and then tends to level out, and that the calcium–sulfur mole ratio is 2.5 after the sulfur fixation efficiency increases and slows down. Sulfur fixation efficiency

attained 28% at a calcium–sulfur mole ratio of 2, and the sulfur fixation efficiency attained 43% at a calcium–sulfur mole ratio of 2.5. At a calcium–sulfur mole ratio of 4.5 sulfur fixation efficiency attained 61%. Because the calcium content of steel slag is relatively low when compared to calcium carbide slag and limestone, adding more steel slag to the coal combustion process will produce a certain amount of ash and reduce the calcium utilization rate; thus, a calcium–sulfur ratio of 2.5 was chosen for this experiment.

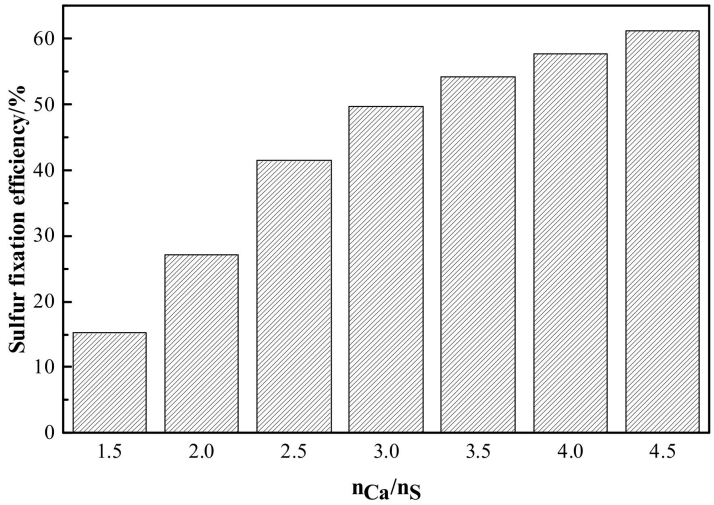

Figure 2. Effect of calcium–sulfur molar ratio on sulfur-fixing efficiency.

3.2. Effect of Single-Factor Additive

The effect of additives on the sulfur fixation performance of steel slag was explored, and the sulfur fixation performance of alkali metal oxides and salts as additives was studied, and it was discovered that sodium lignosulfonate, NaCl, KNO_3, and MnO_2 made a good contribution to the improvement of the sulfur fixation efficiency of steel slag. Figure 2 depicts the impact of the four additions on the slag sulfur fixing efficiency.

Figure 3 depicts the trend of numerous sulfur fixation additives on the sulfur fixation efficiency. The sulfur fixation of steel slag grows first and then drops as the concentration of KNO_3, NaCl, and sodium lignosulfonate increases, while the sulfur fixation efficiency of steel slag increases more quickly and then tends to level out when the content of MnO_2 increases. After high temperature melting, sodium ions in the sulfur-fixing agent surface made a eutectic formation, and the sulfur fixing agent surface ion migration and diffusion ability increased, so as to weaken and improve the sulfur-fixing agent's high temperature sintering. This means that the sulfur-fixing agent surface lattice structure changes and the pore structure increases so that the sulfur-fixing products are not easily blocked by the pores. However, the decomposition temperature of KNO_3 after heating is lower than that of NaCl, which produces oxidation fuel and provides the reactive oxygen required for the sulfur fixation reaction, and the sulfur fixation reaction is carried out in an oxygen-rich atmosphere to further oxidize the intermediate products CaS, $CaSO_3$, etc. to sulfate. The K^+ in it has the same effect as NaCl, and a certain amount of K^+ also changes MnO_2, which decomposes into Mn_2O_3 and Mn_3O_4 during the sulfur fixation reaction [29]; this plays a catalytic function in the sulfur fixation reaction and creates a tiny quantity of Mn_3O_4. Sodium lignosulfonate is put with steel slag to make its particle surface negatively charged, which provides a repulsive attraction between particles, weakening aggregation and delaying sintering, reducing the loss of specific surface area and porosity and facilitating SO_2 absorption.

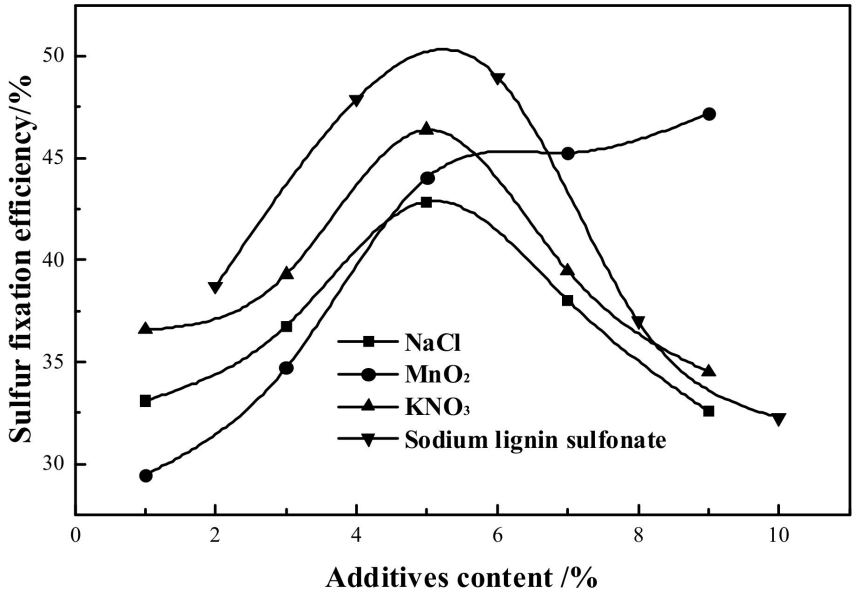

Figure 3. Effect of additive content on sulfur-fixing efficiency.

3.3. Optimization with Orthogonal Experiments

Steel slag was used as the sulfur-fixing agent, and sodium lignosulfonate, KNO_3, NaCl, and MnO_2 were used as four factors (Table 3), with four levels of each factor used to design orthogonal experiments with the sulfur fixation efficiency as the experimental index; the experimental protocol and results analysis are shown in Table 4.

Table 3. Factors and levels of orthogonal experiments.

Level	*w* (Sls)/% (A)	*w* (NaCl)/% (B)	*w* (MnO_2)/% (C)	*w* (KNO_3)/% (D)
1	4	1	1	1
2	6	3	3	3
3	8	5	5	5
4	10	7	7	7

Note: Sls—Sodium lignin sulfonate.

A greater value of the extreme difference R indicates a greater influence of the factor on the experimental results, and vice versa for smaller values. It can be seen from the analysis of the value of the extreme difference R that the order of the factors is A > D > C > B, indicating that the influence of each factor on the performance of the steel slag is A > D > C > B. The most important is sodium lignosulfonate, followed by sodium nitrate, manganese oxide, and sodium chloride, which is rather weak. The greater the average response value k for the same factor, the higher the corresponding level number. According to the order of the influencing factors and the k value, the optimal solution is $A_3B_1C_3D_4$, which is 8% sodium lignosulfonate, 1% NaCl, 5% MnO_2, and 7% KNO_3, and the maximum value of sulfur fixation efficiency from the table of experimental solutions is 70.71%.

Three parallel coal-fired sulfur fixation verification tests were conducted using the optimum scheme of the aforementioned additive ratios, yielding an average sulfur fixation efficiency of 70.81% (70.76%, 71.03%, and 70.64%) for the modified steel slag.

Table 4. Orthogonal experiments plan and experiment results analysis.

Experiment No.	A	B	C	D	Sulfur Fixation Efficiency/%
1	1	1	1	1	48.78
2	1	2	2	2	50.05
3	1	3	3	3	45.25
4	1	4	4	4	50.69
5	2	1	2	3	53.46
6	2	2	1	4	55.45
7	2	3	4	1	59.01
8	2	4	3	2	59.25
9	3	1	3	4	70.71
10	3	2	4	3	55.48
11	3	3	1	2	64.56
12	3	4	2	1	53.41
13	4	1	4	2	54.54
14	4	2	3	1	54.47
15	4	3	2	4	52.21
16	4	4	1	3	51.62
k_1	48.692	56.872	55.103	53.917	
k_2	56.792	53.862	52.282	57.100	
k_3	61.040	55.258	57.420	51.453	
k_4	53.210	53.742	54.930	57.265	
R	12.348	3.130	5.138	5.812	
Sequence	A > D > C > B				
Best scheme	$A_3B_1C_3D_4$				

3.4. Characterization and Analysis

3.4.1. XRF

The composition of the ash was determined using X-ray fluorescence analysis (XRF) on raw coal ash (F_1), sulfur fixation ash of steel slag (F_2), and sulfur fixation ash of modified steel slag (F_3). F_1, F_2, and F_3 are the ashes produced under the same combustion circumstances, and the calcium–sulfur ratios of F_2 and F_3 prior to burning are the same. Table 5 shows how the primary metal components in the sulfur-fixing ash altered with various sulfur-fixing agents and additives, as well as the sulfur concentration of F_1 F_2 F_3. Due to its own sulfur-fixing effect, F_1 contained a small amount of sulfur, and the increased sulfur content of F_2 indicated a stronger sulfur-fixing effect of the slag, and the sulfur content of F_3 was greater than that of F_2, indicating that the additives modified the slag with a stronger sulfur fixation effect.

Table 5. XRF analysis on coal ash.

Ash Sample	*w* (SiO_2)/%	*w* (Al_2O_3)/%	*w* (Fe_2O_3)/%	*w* (CaO)/%	*w* (K_2O)/%	*w* (TiO_2)/%	*w* (SO_3)/%	*w* (MgO)/%	*w* (Na_2O)/%	*w* (MnO)/%
F_1	52.63	30.62	9.20	2.15	1.64	1.29	**0.886**	0.801	0.231	0.0418
F_2	34.55	20.33	17.73	18.05	0.945	1.25	**2.93**	1.27	0.296	1.46
F_3	30.82	17.63	17.31	18.95	2.46	1.21	**4.83**	1.47	1.41	3.75

Note: *w*—Mass fraction.

The mineral composition of the ash is indicated in the form of oxides in the XRF detection analysis findings. The change in CaO concentration in coal ash is significant, and when paired with the SO_3 content analysis, more $CaSO_4$ of sulfur fixation products are found in F_2 and F_3. The greatest percentage of SiO_2 and Al_2O_3 is compatible with the findings of XRD analysis (Figure 4) with greater diffraction peaks in raw coal and the results of $CaAl_2Si_2O_8$ formed during the sulfur fixation process. In F_1, F_2, and F_3, K_2O and

Na_2O as alkali metal oxides have some ionic diffusion influence on the surface crystalline structure of the sulfur fixing agent during the sulfur fixing process, weakening the sintering of the sulfur fixing agent.

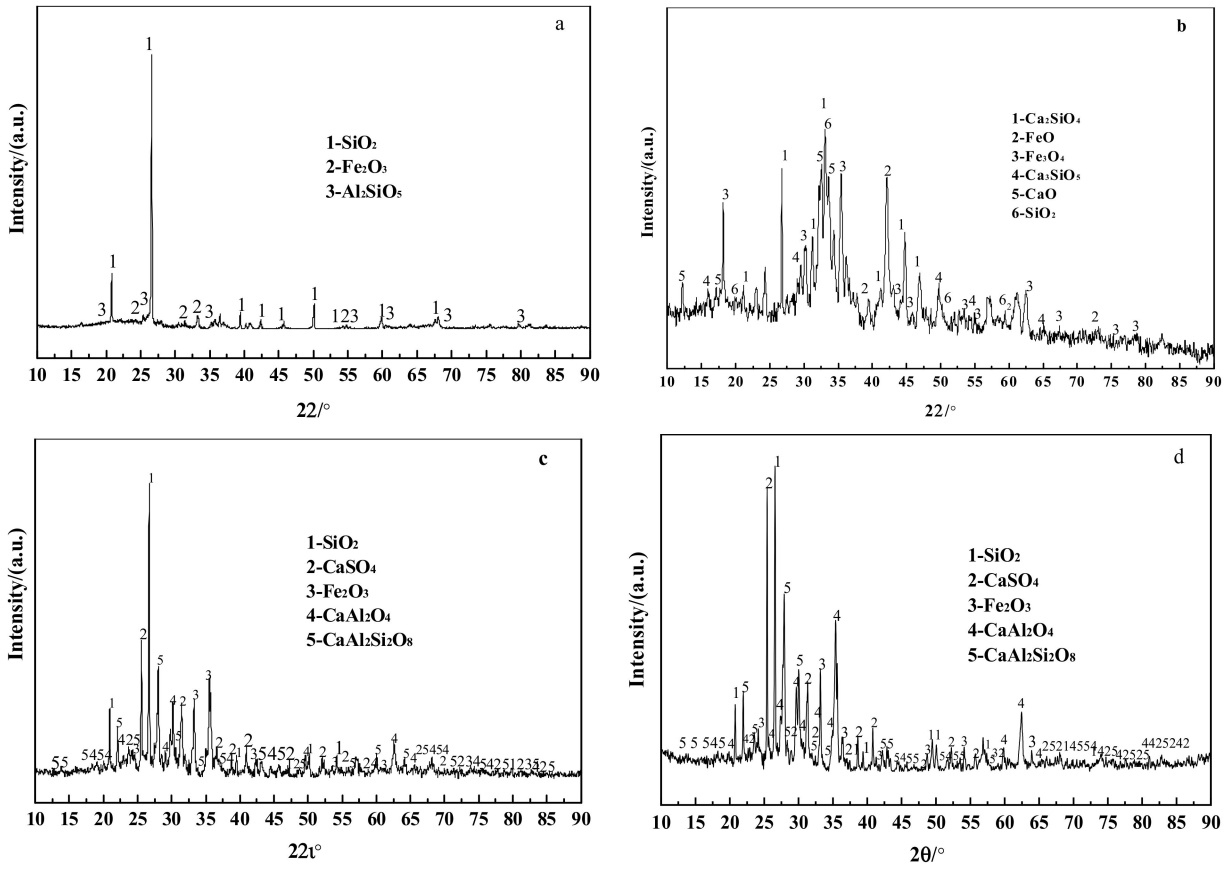

Figure 4. XRD patterns of ash and steel slag. (**a**) F_1; (**b**) Steel slag; (**c**) F_2; (**d**) F_3.

3.4.2. XRD

Figure 4 shows the results of the XRD investigation of F_1, F_2, F_3, and steel slag. F_1 contains more SiO_2, Al_2SiO_5, and Fe_2O_3, and the other alkaline oxides have less content without obvious characteristic peaks, as shown in Figure 4a. Combined with an XRF analysis, the ash is seen to contain a small amount of $CaSO_4$, which is the coal's weak sulfur fixation property, but the products are less. There were no noticeable distinguishing peaks. The steel slag includes more Ca_2SiO_4, Ca_3SiO_5, and iron oxides, as shown in Figure 4b. In combination with the study of steel slag composition in Table 2, a higher amount of CaO in steel slag occurs in the form of Ca_2SiO_4 and Ca_3SiO_5, and only a tiny fraction exists as free CaO. The sulfur fixation reaction of steel slag differs from that of a conventional calcium-based sulfur-fixing agent, and Guo [30] concluded that the sulfur-fixing activity of calcium–silicon sulfur-fixing agent is higher than that of a conventional calcium-based sulfur-fixing agent, and that the sulfur-fixing reaction rate of calcium–silicon sulfur-fixing agent is lower than that of calcium carbonate in the chemical control phase and increases rapidly in the diffusion co-efficient phase.

When comparing Figure 4c,d, the diffraction peaks of $CaSO_4$, a sulfur fixation product, are greatly increased in F_3, indicating that the auxiliary modified steel slag has better sulfur fixation ability. $CaAl_2Si_2O_8$ diffraction peaks are also greatly increased, and more $CaAl_2Si_2O_8$ phase may block sulfur fixation product breakdown and boost sulfur fixing rate. CaO in steel slag and coal ash may readily produce $CaAl_2Si_2O_8$ with Al_2SiO_5 and SiO_2 to avoid $CaSO_4$ breakdown on solid sulfur products at high temperatures. The considerable quantity of $CaAl_2O_4$ mixed with SiO_2 may readily generate

high-temperature resistant silica-aluminate products to prevent sulfur-fixing compounds from decomposing. In the high-temperature molten system of sulfur-fixing ash and coal ash, Al_2SiO_5, $CaAl_2O_4$, $CaAl_2Si_2O_8$, $CaSO_4$, and CaO readily produce sulfoaluminate minerals ($CaO{\cdot}Al_2O_3{\cdot}CaSO_4$), which are high-temperature resistant phases. Spectra include more SiO_2 and Fe_2O_3, and Wu et al. [31]. pointed out that SiO_2 and Fe_2O_3 play a catalytic function in the sulfur fixation process, limiting the high-temperature breakdown of $CaSO_4$, a sulfur fixation product.

3.4.3. SEM

Figure 5 depicts SEM images of F_1, F_2, F_3, steel slag, calcined steel slag, and calcined modified steel slag, revealing their surface morphology and microstructure. In combination with XRD and XRF analysis, Figure 5a depicts the microscopic surface morphology of raw coal ash, which is primarily a mixture of silica and alkali metal oxides, and the coal forms a characteristic loose structure due to gas release and colloidal melting during pyrolysis and combustion. Figure 5b shows a steel slag powder with many dense particles of varied sizes created by various mineral phase crystals formed by the slag during the steelmaking process. In comparison, Figure 5b,c depicts the microscopic surface morphology of steel slag created by high-temperature calcination, and it can be observed that the alkali metal oxides are redistributed on the surface with a greater specific surface area. Figure 5d shows that, following calcination, the modified steel slag extends its specific surface area even more and has a sharp crystal structure connected to the micropores, which may facilitate the sulfur fixation process' reaction.

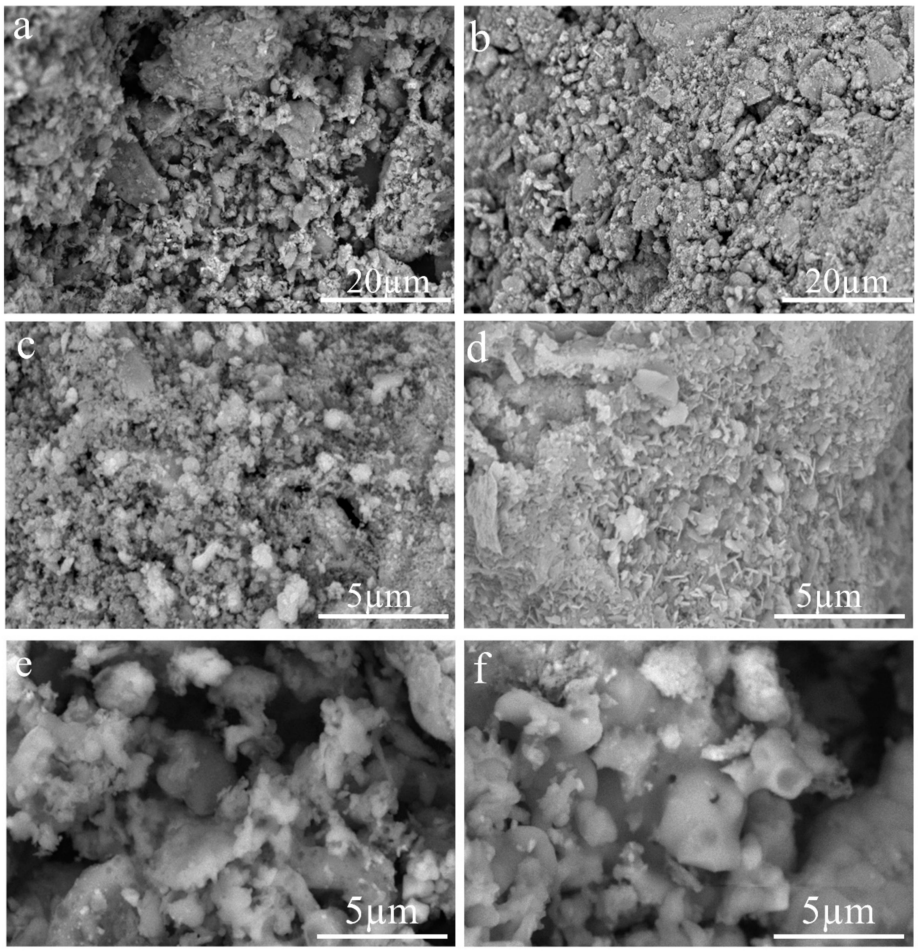

Figure 5. SEM image of coal ash and steel slag. (**a**) Raw coal ash (**b**) Steel slag (**c**) Steel slag after calcination (**d**) Modified steel slag after calcination (**e**) F_2 (**f**) F_3.

Figure 4e compares the ash slag formed by the steel slag after sulfur fixation to Figure 4f—the difference is not obvious, but the ash forms a smoother ablative surface similar to the hot melt at a high temperature, indicating that the steel slag with additives can redistribute the hot melt on the surface of the sulfur-fixing agent during the sulfur fixation process, which can be considered a positive effect. Rather than producing a smooth surface, Figure 4d produces a high specific surface with a sharp, porous, rough structure to promote the sulfur fixation reaction, implying that the addition of additives produced a reaction interface to aid the sulfur fixation process. According to the combined analysis of Figure 4d–f, the addition of additives to the slag provides a good gas–solid reaction interface during the high-temperature sulfur fixation reaction, and the sulfur fixation process proceeds at the interface, forming a new high-temperature resistant phase to inhibit and prevent the decomposition of the sulfur fixation products.

3.5. Mechanism of Sulfur Fixation

The steel slag sulfur-fixing agent undergoes the following reactions during coal combustion.

$$Ca + SO_2 \rightarrow CaSO_3 \quad (2)$$

$$CaSO_3 + 1/2O_2 \rightarrow CaSO_4 \quad (3)$$

$$Ca_2SiO_4 + 2SO_2 + O_2 \rightarrow 2CaSO_4 + SiO_2 \quad (4)$$

$$Ca_3SiO_5 + 3SO_2 + 3/2O_2 \rightarrow 3CaSO_4 + SiO_2 \quad (5)$$

$$CaO + Al_2O_3 \rightarrow CaAl_2O_4 \quad (6)$$

$$CaO + Al_2O_3 + 2SiO_2 \rightarrow CaAl_2Si_2O_8. \quad (7)$$

Steel slag is calcined at high temperatures during coal combustion to form a microscopic structure conducive to SO_2 adsorption, resulting in a certain porosity and specific surface area. The release rate and concentration of SO_2, and the high temperature decomposition of sulfur fixing products, among other factors, determine the sulfur-fixing efficiency. The composite additives promote ion migration and diffusion on the steel slag surface during high temperature calcination, weaken the pore structure of the slag surface sintering at high temperature, change the crystal structure of the slag surface so that SO_2 is easily adsorbed, and promote the generation of a variety of high-temperature resistant substances to coat the sulfur-fixing products and prevent high temperature decomposition. The catalytic impact of the composite additives, on the other hand, lowers the activation energy of the gas–solid interaction, making the sulfur fixation process easier to complete, and the oxidant component in the composite additives promotes complete combustion. The above analysis of the chemical reaction mechanism of sulfur fixation is a reasonable hypothesis.

4. Conclusions and Prospects

(1) The additives have a catalytic effect on the sulfur-fixing reaction of steel slag, as well as forming a microscopic surface structure that promotes the gas–solid reaction and aids in the production of substances that inhibit the decomposition of sulfur-fixing products;

(2) The sulfur fixation efficiency of composite additives modified steel slag is significantly increased, and the optimal amount of additives added at a 1000 °C high temperature is 8% sodium lignosulfonate, 1% NaCl, 5% MnO_2, 7% KNO_3, and the maximum sulfur fixation efficiency of modified steel slag can reach 70.81%;

(3) The XRF, XRD, and SEM investigations revealed that the additive-modified steel slag had higher sulfur fixation performances than the unmodified steel slag and created a material phase that hindered sulfur fixation product breakdown at high temperatures. The surface of the modified steel slag developed morphological characteristics and a microstructure that favored gas–solid interaction;

(4) Because the reaction activity of steel slag is low, future research should focus on finding efficient additives that can increase the sulfur fixation efficiency at low calcium–sulfur ratios. In addition, tempering steel slag and compounding steel slag with other alkali-based solid wastes should be investigated further to lower the cost of sulfur-fixing agents and increase the efficiency of sulfur fixation, allowing steel slag sulfur-fixing agents to be used in a wider range of applications.

Author Contributions: Conceptualization, J.Z. and Q.Y.; Formal analysis, J.Z.; Funding acquisition, Q.Y.; Methodology, J.Z. and X.W.; data curation, M.L.; Writing, J.Z. All authors have read and agreed to the published version of the manuscript.

Funding: This research was funded by the Beijing Science and Technology Plan Funding Project (Z161100002616038) and Central universities basic research business expenses special funds (2020YJSHH24).

Institutional Review Board Statement: Not applicable.

Informed Consent Statement: Not applicable.

Data Availability Statement: The data presented in this study are available on request from the corresponding author.

Acknowledgments: We gratefully acknowledge support from the School of Chemical and Environmental Engineering, China University of Mining and Technology-Beijing.

Conflicts of Interest: The authors declare no conflict of interest.

References

1. Jiang, L.; He, S.; Zhou, H.; Kong, H.; Wang, J.; Cui, Y.; Wang, L. Coordination between sulfur dioxide pollution control and rapid economic growth in China: Evidence from satellite observations and spatial econometric models. *Struct. Chang. Econ. Dyn.* **2021**, *57*, 279–291. [CrossRef]
2. Pang, L.; Shao, Y.J.; Zhong, W.Q.; Liu, H. Oxy-coal combustion in a 30 kW(th) pressurized fluidized bed: Effect of combustion pressure on combustion performance, pollutant emissions and desulfurization. *Proc. Combust. Inst.* **2021**, *38*, 4121–4129. [CrossRef]
3. Meng, J.; Wang, J.; Yang, F.; Hao, Y.; Cheng, F. Effects of Sulfur-fixing Agent on Coal Combustion Characteristics and S, N Release Law in Condition of Lean Oxygen. *Coal Convers.* **2020**, *43*, 27–37.
4. Wichliński, M.; Włodarczyk, R. Assessment of the Impact of Modification of Calcium Sorbents and the Possibility of Their Use in Desulfurization for Oxy-Fuel Combustion Process. *Minerals* **2021**, *11*, 1284. [CrossRef]
5. Chu, S.; Zhu, C.; Tompsett, G.A.; Mountziaris, T.J.; Dauenhauer, P.J. Refuse-Derived Fuel and Integrated Calcium Hydroxide Sorbent for Coal Combustion Desulfurization. *Ind. Eng. Chem. Res.* **2015**, *54*, 3136–3144. [CrossRef]
6. Pang, L.; Shao, Y.J.; Zhong, W.Q.; Liu, H. Experimental study of SO_2 emissions and desulfurization of oxy-coal combustion in a 30 kW(th) pressurized fluidized bed combustor. *Fuel* **2020**, *264*, 116795. [CrossRef]
7. Kim, Y.B.; Gwak, Y.R.; Keel, S.I.; Yun, J.H.; Lee, S.H. Direct desulfurization of limestones under oxy-circulating fluidized bed combustion conditions. *Chem. Eng. J.* **2019**, *377*, 119650. [CrossRef]
8. Luo, M.; Zhou, L.; Wang, C.; Kuang, C. The evolution and desulfurization of sulfur in chemical looping combustion of coal. *Energy Sources Part A Recover. Util. Environ. Eff.* **2021**, 1–12. [CrossRef]
9. Liu, Y.; Zhou, F.-S.; Hu, Y.-M.; Zhang, Y.-H. Sulfur Fixation by Chemically Modified Red Mud Samples Containing Inorganic Additives: A Parametric Study. *Adv. Mater. Sci. Eng.* **2016**, *2016*, 9817969. [CrossRef]
10. Zhao, G.J.; Yin, F.J.; Li, J.; Li, X.Y. Study on Pore Structure and Sulfur Fixation Characteristics of Alkali Industrial Waste. *Adv. Mater. Res.* **2011**, *194-196*, 716–721. [CrossRef]
11. Zhao, G.; Shi, Y.; Ni, C.; Lu, C.; Yin, F.; Wu, J.; Sheng, C. Notice of Retraction: The Influence Mechanism of Rapid Hydration Drying on Medium Temperature Sulfur Fixation Performance of Alkali Industrial Waste. In Proceedings of the 2010 4th International Conference on Bioinformatics and Biomedical Engineering, Chengdu, China, 18–20 June 2010; pp. 1–4. [CrossRef]
12. Guo, Y.X.; Li, Y.T.; Cheng, F.Q.; Yang, F.L. Effect of Coal Fly Ash as Additive on the Sulfur Retention of Coal Briquette. *Adv. Mater. Res.* **2012**, *512–515*, 1583–1588. [CrossRef]
13. Gao, Y.; Yang, Y.; Zhu, G.; Deng, N. Improving the efficiency of CaO-based sorbent by $SrCO_3$ for high-temperature sulfur removal during coal combustion. *Green Processing Synth.* **2017**, *6*, 577–582. [CrossRef]
14. Okura, T.; Ueda, S.; Yamaguchi, K. Elemental sulphur fixation in smelting gas; Is it feasible? *Sohn Int. Symp. Adv. Processing Met. Mater.* **2006**, *8*, 425–431.
15. Zhao, Y.; Wang, S.Q.; Shen, Y.M.; Lu, X.J. Effects of nano-TiO_2 on combustion and desulfurization. *Energy* **2013**, *56*, 25–30. [CrossRef]

16. Wang, S.-Q.; Liu, M.-Z.; Sun, L.-L.; Cheng, W.-L. Study on the mechanism of desulfurization and denitrification catalyzed by TiO_2 in the combustion with biomass and coal. *Korean J. Chem. Eng.* **2017**, *34*, 1882–1888. [CrossRef]
17. Brand, A.S.; Fanijo, E.O. A Review of the Influence of Steel Furnace Slag Type on the Properties of Cementitious Composites. *Appl. Sci.* **2020**, *10*, 8210. [CrossRef]
18. Chand, S.; Paul, B.; Kumar, M. Sustainable Approaches for LD Slag Waste Management in Steel Industries: A Review. *Metallurgist* **2016**, *60*, 116–128. [CrossRef]
19. Jiang, Y.; Ling, T.-C.; Shi, C.; Pan, S.-Y. Characteristics of steel slags and their use in cement and concrete—A review. *Resour. Conserv. Recycl.* **2018**, *136*, 187–197. [CrossRef]
20. Weng, Y.; Liu, Y.; Liu, J. Study on mathematical model of hydration expansion of steel slag-cement composite cementitious material. *Environ. Technol.* **2021**, *42*, 2776–2783. [CrossRef]
21. Jafari, A.J.; Moslemzadeh, M. Investigation of phosphorus removal using steel slag from aqueous solutions: A systematic review study. *Int. J. Environ. Anal. Chem.* **2020**, *102*, 821–833. [CrossRef]
22. Dhoble, Y.N.; Ahmed, S. Review on the innovative uses of steel slag for waste minimization. *J. Mater. Cycles Waste Manag.* **2018**, *20*, 1373–1382. [CrossRef]
23. Yang, L.; Wei, T.; Li, S.; Lv, Y.; Miki, T.; Yang, L.; Nagasaka, T. Immobilization persistence of Cu, Cr, Pb, Zn ions by the addition of steel slag in acidic contaminated mine soil. *J. Hazard. Mater.* **2021**, *412*, 125176. [CrossRef] [PubMed]
24. Gao, D.; Wang, F.P.; Wang, Y.T.; Zeng, Y.N. Sustainable Utilization of Steel Slag from Traditional Industry and Agriculture to Catalysis. *Sustainability* **2020**, *12*, 9295. [CrossRef]
25. Kang, L.; Du, H.L.; Zhang, H.; Ma, W.L. Systematic Research on the Application of Steel Slag Resources under the Background of Big Data. *Complexity* **2018**, *2018*, 6703908. [CrossRef]
26. Guo, J.; Bao, Y.; Wang, M. Steel Slag in China: Treatment, Recycling, and Management. *Waste Manag.* **2018**, *78*, 318–330. [CrossRef] [PubMed]
27. Herbelin, M.; Bascou, J.; Lavastre, V.; Guillaume, D.; Benbakkar, M.; Peuble, S.; Baron, J.P. Steel Slag Characterisation Benefit of Coupling Chemical, Mineralogical and Magnetic Techniques. *Minerals* **2020**, *10*, 705. [CrossRef]
28. Neveux, T.; Hagi, H.; Le Moullec, Y. Performance simulation of full-scale wet flue gas desulfurization for oxy-coal com-bustion. *Energy Procedia* **2014**, *63*, 463–470. [CrossRef]
29. Zhang, S.; Xie, B. Influence of MnO_2 for CaO in coal powder combustion. *Chin. J. Environ. Eng.* **2012**, *6*, 4157–4161.
30. Guo, F.; Wu, Z.; Cui, A.; Wang, L. Desulfurization and Kinetic Studies on $CaCO_3$-SiO_2 Complex Desulfurization Reagent. *Chem. J. Chin. Univ.* **2003**, *1*, 100–104.
31. Wu, J.; Yang, X.; Han, J.; Chen, T. Prohibition of $CaSO_4$ decomposition at high temperature by oxides/carbonates additives. *J. China Univ. Min. Technol.* **2005**, *4*, 660–663.